

Reversible formation of hybrid nanostructures *via* an organic linkage†

Liangfei Tian, Chunsheng Shi and Jin Zhu*

Received (in Cambridge, UK) 8th May 2007, Accepted 29th June 2007

First published as an Advance Article on the web 18th July 2007

DOI: 10.1039/b706889a

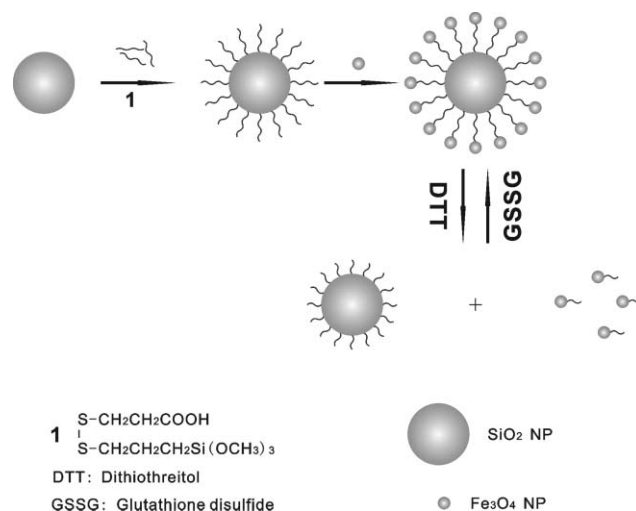
A reversible formation of hybrid nanostructures has been successfully achieved *via* an organic linker containing a cleavable disulfide bond, which provides a general route to the preparation of controllable composite architectures using particles of distinct compositions.

Hybrid nanostructures offer distinct properties that are different from the constituent components. The superior properties derive from properly configured spatial distribution of chemical structures with desired compositions. Spatially resolved hybrid type architectures comprised of core and shell layers, with programmable structural parameters for each individual building block, have proven especially useful in conferring precisely defined and tailorable functional properties upon the fabricated composite materials.¹ Indeed, they have contributed to the development of designer nanostructures targeting a broad spectrum of applications.² The construction of such hybrid nanostructures typically involves controlled deposition of a shell layer on template cores, through either direct reactions from molecular precursors or self-assembly from preformed building blocks.¹ The latter strategy, which builds upon complementary surface recognition elements for interactions, has demonstrated its versatility in controlling the architectures of hybrid nanostructures through organic and biological interconnects.³ The ability to control the capture and release of shell layers would enable one to deliberately turn on and off the unique properties offered by such materials. Herein we report the reversible formation of hybrid nanostructures through an organic linkage. Our methodology relies on the use of a molecule that affords switchable covalent connectivity under different chemical environments.

Two types of nanoparticles (NPs) are employed in the initial proof-of-concept demonstration reported herein: SiO₂ NPs in the sub-micrometer size range, and Fe₃O₄ NPs with a much smaller physical dimension, Scheme 1. The substantial size difference allows facile characterization of the hybrid nanostructures with transmission electron microscopy (TEM). Key to the success of our strategy lies in the design of an organic linker molecule, 2-[3-(trimethoxysilyl)propyl]disulfany]propionic acid (**1**), which possesses three functional groups: a trimethoxysilyl group at one end,

a carboxylic group at the other end, and a disulfide linkage at the center. Our hybrid nanostructure assembly strategy takes advantage of initially preferred reaction between the trimethoxysilyl group of **1** and hydroxyl groups on SiO₂ NP surfaces.⁴ After this step, the carboxylic group is exposed on the monolayer-modified SiO₂ NPs, which can interact with Fe₃O₄ NPs under carefully chosen conditions, affording hybrid nanostructures. The central disulfide bond can undergo cleavage in the presence of DTT, leading to the formation of thiol groups on both SiO₂ and Fe₃O₄ NP surfaces and simultaneous release of the shell layer. The reformation of hybrid nanostructure can be effected by GSSG, an oxidant that is typically adopted in the conversion of thiol to disulfide. Our experiments show that the functional groups within the organic linkers that bridge SiO₂ and Fe₃O₄ NPs are accessible to external reagents for chemical transformations, and that, despite the existence of a significant number of linkages in close proximity between NPs, the release of shell NPs is highly effective. Prior to this work, major efforts have been focused on exploiting non-covalent molecular recognitions for the manipulation of heterostructures.^{5,6}

The linker molecule **1** was synthesized according to a two-step procedure.⁷ SiO₂ NPs with an average diameter of 400 nm were prepared *via* the Stöber method,⁸ and allowed to react with **1** for 12 h. Isolation of functionalized NPs was achieved by repeated centrifugation, decanting and redispersion in ethanol. The powder was dried overnight at 100 °C to remove residual solvent. Fe₃O₄ NPs were prepared by following a literature protocol.⁹ The as-prepared Fe₃O₄ NPs were purified by magnetic separation and dialysis against H₂O. TEM analysis showed that Fe₃O₄ NPs were not perfectly dispersed and a networked structure could be



Scheme 1

Department of Polymer Science and Engineering, School of Chemistry and Chemical Engineering, State Key Laboratory of Coordination Chemistry, Nanjing University, Nanjing, 210-093, China.
 E-mail: jinz@nju.edu.cn; Fax: +86-25-8331-7761;
 Tel: +86-25-8368-6291

† Electronic supplementary information (ESI) available: Experimental section. Fig. S1: TEM images of the possible Fe₃O₄ NP dimers. Fig. S2: TEM image of SiO₂-Fe₃O₄ hybrid nanostructures after butyric acid treatment. Fig. S3: TEM image of as-prepared Fe₃O₄ NPs. Fig. S4: ζ potential of Fe₃O₄ and SiO₂ NPs at different pH values. See DOI: 10.1039/b706889a

observed. The aggregation behavior of Fe_3O_4 NPs poses a substantially greater challenge for their release compared with gold NPs (see below).⁶ To effect the assembly of Fe_3O_4 NPs on functionalized SiO_2 NPs, electrostatic interactions were employed. This was done by carefully examining the ζ -potentials of bare Fe_3O_4 NPs and modified SiO_2 NPs at different pHs. At pH 5, the negative charge on modified SiO_2 NPs complements the positive charge on Fe_3O_4 NPs, allowing electrostatic interactions to take place. Therefore, when the functionalized SiO_2 NPs were mixed with Fe_3O_4 NPs at pH 5 in a hexamethylenetetramine–HCl (10 mM) buffer for 12 h, extensive hybrid nanostructures were observed (Fig. 1(a) and (b)). In this particular case, it is difficult to quantify the exact number of shell Fe_3O_4 NPs due to the existence of closely spaced NPs. Scanning electron microscopy (SEM) further confirmed the existence of the structures (Fig. 2(a)). Several experimental observations that are crucial for achieving the hybrid nanostructures deserve comment: the formation of hybrid nanostructures require the utility of a buffer that does not contain functional groups interacting with Fe_3O_4 NP surfaces. In this regard, phosphate and acetate buffers failed to afford the same type of heterostructures under otherwise identical conditions. Instead, Fe_3O_4 NPs, separating from SiO_2 NPs, formed very disorganized, random aggregates. In addition, a high ionic strength would disrupt the interactions between the carboxylic groups and

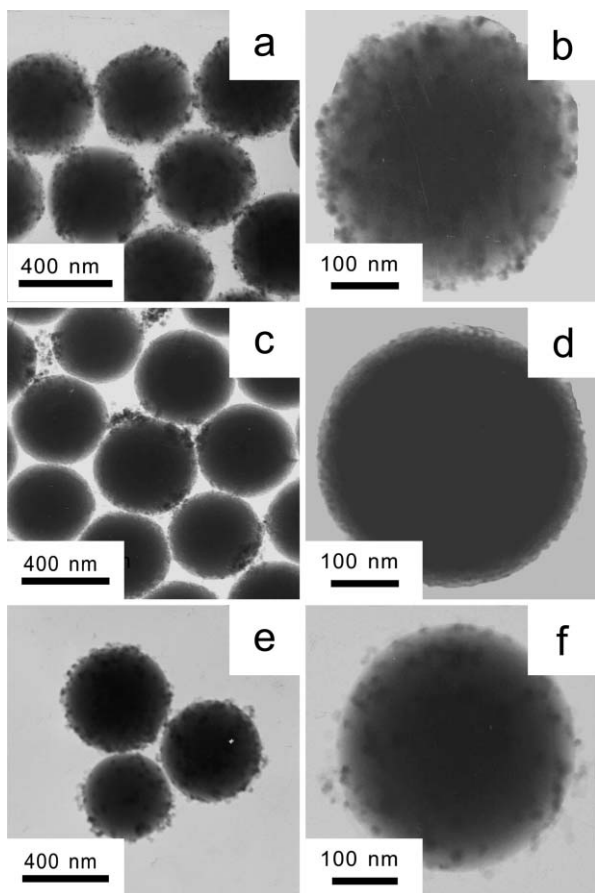


Fig. 1 TEM images of SiO_2 - Fe_3O_4 hybrid nanostructures. ((a) and (b)) Hybrid structures of Fe_3O_4 and SiO_2 NPs. ((c) and (d)) The shell-released structures after DTT treatment. ((e) and (f)) The reformation of hybrid structures after GSSG treatment.

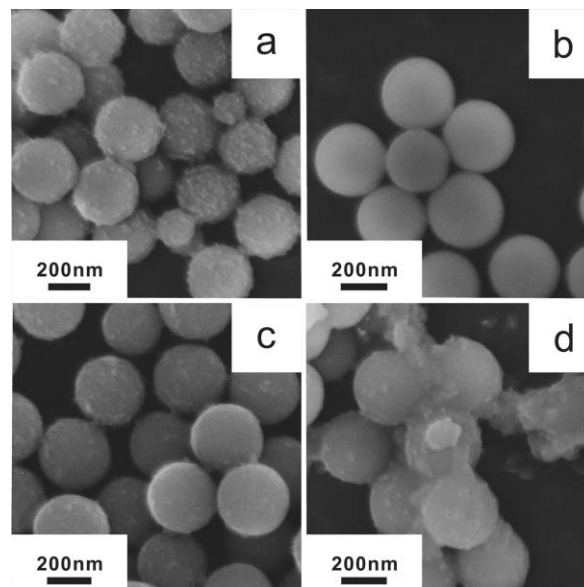


Fig. 2 SEM images of the hybrid nanostructures. (a) Hybrid structure of Fe_3O_4 and SiO_2 NPs. (b) The shell-released structures after DTT treatment. (c) The reformation of hybrid structure after GSSG treatment. (d) Gold NPs captured on shell-released SiO_2 NPs. Note that the small amount of irregularly shaped material in (d) is likely from organic molecules.

Fe_3O_4 NP surfaces, resulting in poorly structured shell layers. Significantly, once the hybrid assemblies are constructed, a change of pH would not lead to the dissociation of shell layer.

As depicted in Scheme 1, release of Fe_3O_4 NPs was accomplished using DTT.¹⁰ The shell-release process is a complex phenomenon, complicated by the participation of several interacting components. We hypothesized that aggregation of Fe_3O_4 NPs, due to the large surface area, would inhibit the dissociation of cleaved shell structures. This could be circumvented by the surface modification with a small molecule. Butyric acid proved to be useful in this regard and accelerated the shell dissociation process, with the assistance of sonication. The accelerating effect of butyric acid is accomplished by interacting and capping part of the Fe_3O_4 NP surface that has not been occupied by the linker molecule, which directly leads to a significant reduction in the interaction between the bare Fe_3O_4 NP surfaces. There are multiple linkages formed between the Fe_3O_4 NPs and SiO_2 NPs by the organic linker. Due to the multi-valent effect, the butyric acid could not displace the organic linker. Thus, an evaluation of the effect of concentration suggested that 10 mM was optimum for achieving the purpose. To this end, the hybrid nanostructures were incubated in a butyric acid solution (pH 5) for 12 h. Because oxygen was detrimental to the reaction, the NP solution was bubbled with argon for 15 min before the addition of DTT. Then the mixture was rotated for 12 h to ensure the completeness of the reaction. TEM analysis of the sample revealed that the reaction was effective and Fe_3O_4 NPs were successfully cleaved off the SiO_2 NP surfaces (Fig. 1(c) and (d)). Slight amount of residual Fe_3O_4 NPs were also observed surrounding SiO_2 NPs, presumably due to non-specific interactions or the solvent evaporation-induced aggregation between the two NPs on the Cu grid. SEM observation allowed us to confirm the existence of virtually shell layer-free SiO_2

NPs (Fig. 2(b)). A control experiment carried out in the absence of butyric acid led to an extremely low efficiency in the release of the shell layer.

To further demonstrate that the disulfide bond has been effectively cleaved, in accordance with Scheme 1, we selected GSSG,¹¹ a mild oxidant that would not react with other functional groups within molecule **1**, to effect reformation of the covalent bond. To achieve this, we first completely removed DTT from the system by successive centrifugation and redispersion three times with H₂O, then redispersed the material in a hexamethylenetetramine-HCl (pH 5, 10 mM) buffer solution. Following the addition of GSSG, the mixture was left rotating for 12 h. After this step, the reversible formation of the hybrid assembly was achieved, as evidenced by TEM (Fig. 1(e) and (f)). SEM observation allowed us to reach the same conclusion (Fig. 2(c)). In addition to the participation of GSSG, the hybrid reformation could only be accounted for by taking into consideration several other factors: the significant size and concentration difference between the two types of NPs, and the asymmetrical modification of Fe₃O₄ NPs. First, because SiO₂ NPs have a larger surface and are uniformly modified with thiol groups, statistically Fe₃O₄ NPs have a higher probability to get in contact with the SiO₂ NPs. Second, Fe₃O₄ NPs, due to their physical size and asymmetrically modified surfaces, have a lower chance to form inter-particle dimers. Lastly, because of less amount and less significant Brownian motion of SiO₂ NPs compared with Fe₃O₄ NPs, the possibility of the collision between SiO₂ NPs is much smaller, SiO₂ NPs could hardly form aggregates. Some dissociated and aggregated Fe₃O₄ NPs could still be identified on the Cu grid. This could be caused by the burial of thiol groups within aggregated Fe₃O₄ NPs, rendering them inaccessible for reaction with GSSG, or the intermolecular disulfide bond formation on the same NP surface upon GSSG oxidation. This leads to the lower surface coverage of shell material in the reformed hybrid nanostructure (Fig. 1(b) and (f)). Another factor that should be taken into account is the loss of Fe₃O₄ NPs during the centrifugation/washing step. It is interesting to note that some Fe₃O₄ NPs formed dimers (Fig. 1S, ESI[†]), indicative of the formation of disulfide bond.

Moreover, we reasoned that, if the disulfide bond was successfully cleaved, thiol groups left on SiO₂ NPs and Fe₃O₄ NPs could be utilized for the directed synthesis of other heterostructures. Gold NPs, which could form strong coordination bonds with thiols, were employed to evaluate the feasibility of the idea. Indeed, with the addition of gold NPs under sonication conditions, a substantial percentage of SiO₂ particles were modified with gold NPs (Fig. 3(a) and (b)), which was also substantiated by SEM (Fig. 2(d)). Further, Fe₃O₄ NPs, due to their locally modified surfaces, formed oligomeric structures with gold NPs, instead of extended networks (Fig. 3(c) and (d)). A change of the ratio between Fe₃O₄ and gold NPs invariably resulted in the identification of similar structures.

In summary, we have successfully achieved the reversible formation of hybrid nanostructures by utilizing an organic linker containing cleavable disulfide bond. The strategy could be easily extended to a vast array of NPs with varied compositions, sizes and other structural parameters. Future work will be focused on the demonstration of this assembly scheme in the reversible control of functions.

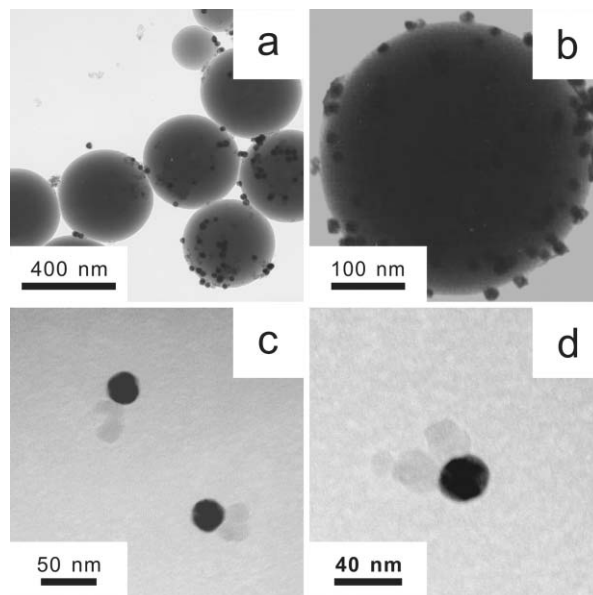


Fig. 3 ((a) and (b)) TEM images of the gold NPs captured on SiO₂ NPs. ((c) and (d)) Gold NPs assembled with Fe₃O₄ NPs; note that the dark-contrasted NPs are gold, while the light-contrasted NPs are Fe₃O₄.

J. Z. acknowledges support from the National Natural Science Foundation of China (20604011), the National Basic Research Program of China (2007CB925103), and the Program for New Century Excellent Talents in University (NCET-06-0451).

Notes and references

- 1 F. Caruso, *Adv. Mater.*, 2001, **13**, 11.
- 2 (a) V. Salgueirino-Maceira, F. Caruso and L. M. Liz Marzán, *J. Phys. Chem. B*, 2003, **107**, 10990; (b) C.-W. Chen, T. Serizawa and M. Akashi, *Chem. Mater.*, 1999, **11**, 1381; (c) A. Rogach, A. Susha, F. Caruso, G. Sukhorukov, A. Kornowski, S. Kershaw, H. Möhwald, A. Eychmüller and H. Weller, *Adv. Mater.*, 2000, **12**, 333.
- 3 (a) F. Caruso, S. A. Susha, M. Giersig and H. Möhwald, *Adv. Mater.*, 1999, **11**, 950; (b) F. Caruso, M. Spasova, A. Susha, M. Giersig and R. A. Caruso, *Chem. Mater.*, 2001, **13**, 109; (c) R. C. Mucic, J. J. Storhoff, C. A. Mirkin and R. L. Letsinger, *J. Am. Chem. Soc.*, 1998, **120**, 12674.
- 4 L. Wang, J. Luo, Q. Fan, M. Suzuki, I. S. Suzuki, M. H. Engelhard, Y. Lin, N. Kim, J. Q. Wang and C.-J. Zhong, *J. Phys. Chem. B*, 2005, **109**, 21593.
- 5 (a) C. A. Mirkin, *Inorg. Chem.*, 2000, **39**, 2258; (b) X. Xu, N. L. Rosi, Y. Wang, F. Huo and C. A. Mirkin, *J. Am. Chem. Soc.*, 2006, **128**, 9286.
- 6 For asymmetric functionalization of gold NPs via a cleavable covalent bond, see: (a) K.-M. Soon, D. W. Mosley, B. R. Peelle, S. Zhang and J. M. Jacobson, *J. Am. Chem. Soc.*, 2004, **126**, 5064; (b) J. G. Worden, A. W. Shaffer and Q. Huo, *Chem. Commun.*, 2004, 518; (c) B. Li and C. Y. Li, *J. Am. Chem. Soc.*, 2007, **129**, 12. For reversible binding of gold NPs on solid supports via a covalent linkage, see: (d) O. Abed, M. Wanunu, A. Vaskevich, R. Arad-Yellin, A. Shanzler and I. Rubinstein, *Chem. Mater.*, 2006, **118**, 1247. For pH-controlled manipulation of hybrid nanoparticles, see: (e) H. Hiramatsu and F. E. Osterloh, *Langmuir*, 2003, **19**, 7003.
- 7 D. R. Radu, C.-Y. La, J. Huang, X. Shu and V. S.-Y. Lin, *Chem. Commun.*, 2005, 1264.
- 8 W. Stöber, A. Fink and E. Bohn, *J. Colloid Interface Sci.*, 1968, **26**, 62.
- 9 A. Chen, H. Wang, B. Zhao and X. Li, *Synth. Met.*, 2003, **139**, 411.
- 10 W. W. Cleland, *Biochemistry*, 1964, **3**, 480.
- 11 M. Narayan, E. Welker, W. J. Wedemeyer and H. A. Scheraga, *Acc. Chem. Res.*, 2000, **33**, 805.